eprints@whiterose.ac.uk
https://eprints.whiterose.ac.uk/

Scaling Transform Based Information Geometry Method for DOA Estimation

Yang-Yang Dong, Chun-Xi Dong, Wei Liu, *Senior Member, IEEE*, Ming-Ming Liu, and Zheng-Zhao Tang

Abstract

By exploiting the relationship between probability density and the differential geometry structure of received data and geodesic distance, the recently proposed information geometry (IG) method can provide higher accuracy and resolution ability for direction of arrival (DOA) estimation than many existing methods. However, its performance is not robust even for high signal to noise ratio (SNR). To have a deep understanding of its unstable performance, a theoretical analysis of the IG method is presented by deriving the relationship between the cost function and the number of array elements, powers and DOAs of source signals, and noise power. Then, to make better use of the nonlinear and super resolution property of the cost function, a Scaling TRansform based INformation Geometry (STRING) method is proposed, which simply scales the array received data or its covariance matrix by a real number. However, the expression for the optimum value of the scalar is complicated and related to the unknown signal DOAs and powers. Hence, a decision criterion and a simple search based procedure are developed, guaranteeing a robust performance. As demonstrated by computer simulations, the proposed STRING method has the best and robust angle resolution performance compared with many existing high resolution methods and even outperforms the classic Cramer-Rao bound (CRB), although at the cost of a bias in the estimation results.

Index Terms

direction of arrival estimation, information geometry, scaling transform, STRING.

I. INTRODUCTION

Direction of arrival (DOA) estimation for multiple sources has very important applications including wireless communications, radar, sonar, and electronic reconnaissance, etc [1]–[3]. The key property of modern DOA estimation methods is their ability to resolve sources placed spatially within the Rayleigh resolution of a sensor array. These methods are often called as high resolution even super resolution methods and can be classified

into three main approaches. The first is subspace based method assuming source signals and noise are located in two orthogonal subspaces, such as multiple signal classification (MUSIC) [4], estimation of signal parameters via rotational invariance technique (ESPRIT) [5], and the propagator method (PM) [6]. For the second approach, it treats DOA estimation as a data fitting problem and two representative methods are maximum likelihood (ML) [7]–[10] and subspace fitting (SF) [11], [12]. Since they normally require multidimensional search or nonlinear optimization with a very high computational cost, many computationally efficient methods have been developed, such as alternating projection (AP) [13], expectation maximization (EM) [14], iterative quadratic maximum likelihood (IQML) [15], [16], and iterative method of direction estimation (IMODE) [17]. The third approach is based on sparse representation, which treats DOA estimation as a sparse recovery problem [18]–[21].

To improve the DOA estimation performance beyond these classic approaches, many methods have utilized different properties of source signals and array geometry, such as higher order statistics [22], [23], quasi-stationary signals [24]–[26], non-circular source signals [18], [27]–[29], nested or co-prime arrays [26], [30], [31], et al. However, utilization of these special properties also means their application is restricted and less general.

Most recently, a new approach for DOA estimation was introduced based on information geometry (IG) [32], which can provide a higher resolution than conventional methods without placing strong constraints on properties of source signals and array geometry. As discussed in [33], the cone of the covariance matrix is not a vector space and the utilization of other distances, e.g., Euclidean distance, may result in performance degradation. The core idea of the IG method is to establish an optimization problem by exploiting the geodesic distance criterion and solving it using linear search, and an additional benefit is that it can handle the underdetermined case. However, its performance is sensitive to the value of noise and source signal powers in addition to the signal to noise ratio (SNR), and it may not give effective estimates even for a high SNR.

To have a more consistent performance while keeping its high resolution, in this work, we first give an analysis to the IG method and derive the analytical expression for the IG spectrum cost function with respect to the number of array elements, signal and noise power, and source DOAs for single and two sources cases, where their values have a great effect on the estimation performance and may cause failure of the method. Then, considering the nonlinear relationship between the IG spectrum cost function and these parameters, a simple Scaling TRansform based INformation Geometry (STRING) method is proposed, which can change the value of the original cost function and generate peaks at true DOAs. Specifically, the optimum scaling coefficients are derived for single and two closely spaced sources. However, the optimum scaling coefficient is complicated and related to unknown DOAs and unknown source signal and noise powers. Therefore, a linear search based approach is proposed for finding the optimum scaling coefficient to provide a condition for high resolution and stable estimation performance. As shown by computer simulations, the proposed method outperforms the existing ones and the classic Cramer-Rao bound (CRB), although at the cost of a bias in the estimation results.

The remaining parts of the paper are organized as follows. In Section 2, the signal model is introduced and an analysis of the IG method is performed in Section 3, while the proposed estimation method is presented in Section 4. Simulation results are provided in Section 5 and conclusions are drawn in Section 6.

Notations: matrices and vectors are denoted by boldfaced capital letters and lower-case letters, respectively. $(\cdot)^*$, $(\cdot)^T$ $(\cdot)^H$, and $(\cdot)^{-1}$ stand for conjugate, transpose, conjugate transpose, and inverse, respectively. $E\{\cdot\}$, $\mathrm{diag}\{\cdot\}$, $|\cdot|$, and $\mathrm{tr}\{\cdot\}$ denote the statistical expectation, diagonalization, amplitude of a complex number, and the trace of a square matrix, respectively.

II. Signal model

Consider an M-element uniform linear array (ULA) with interspacing d and assume there are K uncorrelated narrowband far-field sources with wavelength λ impinging from directions $\boldsymbol{\theta} = [\theta_1, \theta_2, \cdots, \theta_K]^T$. The received signal vector of the ULA at the nth snapshot ($n = 1, 2, \cdots, N$) can be represented by

$$\mathbf{x}(n) = \mathbf{A}(\boldsymbol{\theta})\mathbf{s}(n) + \mathbf{w}(n) \tag{1}$$

where $\mathbf{A}(\boldsymbol{\theta}) = [\mathbf{a}(\theta_1), \mathbf{a}(\theta_2), \cdots, \mathbf{a}(\theta_K)]$, $\mathbf{a}(\theta_k) = [1, z_k, \cdots, z_k^{M-1}]$, and $z_k = \exp(-j2\pi d \sin\theta_k/\lambda)$. Since the source signals are uncorrelated, $E\{\mathbf{s}(n)\mathbf{s}^H(n)\} = \mathrm{diag}\{p_1, p_2, \cdots, p_K\}$. The noise signals are considered to be independent and identically distributed (i.i.d.) complex Gaussian, i.e., $\mathbf{w}(n) \sim CN(\mathbf{0}, \sigma_w^2 \mathbf{I}_M)$, and uncorrelated with signals.

III. Analysis of the IG method

A. Brief review of the IG method

For the IG method, using the principle of information geometry, the DOA estimation problem can be transformed into the following optimization problem [32],

$$\min_{\tilde{\mathbf{R}}, \tilde{\mathbf{A}}(\boldsymbol{\theta}) \in \mathbb{A}} d_G(\mathbf{R}_{xx}, \tilde{\mathbf{R}}) \ \ s.t. \ \tilde{\mathbf{R}} = \tilde{\mathbf{A}}(\boldsymbol{\theta})\tilde{\mathbf{A}}(\boldsymbol{\theta})^H \tag{2}$$

where $\mathbb{A}$ is the set of feasible array manifold matrices, and the covariance matrix is $\mathbf{R}_{xx} = E\{\mathbf{x}(n)\mathbf{x}^H(n)\} = \sum_{k=1}^{K} p_k \mathbf{a}(\theta_k)\mathbf{a}^H(\theta_k) + \sigma_w^2 \mathbf{I}_M$. The notation $d_G(\cdot, \cdot)$ represents the IG distance and $d_G(\mathbf{R}_{xx}, \tilde{\mathbf{R}}) = \sum_{m=1}^{M} (\log \varsigma_m)^2$, where $\{\varsigma_m\}_{m=1}^{M}$ are the eigenvalues given by the generalized eigenvalue decomposition (GEVD) of $\mathbf{R}_{xx}$ and $\tilde{\mathbf{R}}$.

It is noticed that (2) can be solved via multidimensional search with a high computational complexity. To reduce it, Coutino et al. transformed it into the following rank-one problem [32],

$$\max_{\theta \in [-90^\circ, 90^\circ]} f(\theta) = 1/d_G(\mathbf{R}_{xx}, \tilde{\mathbf{R}}(\theta)) \tag{3}$$

where $\tilde{\mathbf{R}}(\theta) = \mathbf{a}(\theta)\mathbf{a}^H(\theta)$. (3) is the optimization problem of the IG-Pencil method and can be solved easily with a simple linear search.

Additionally, Coutino et al's proved that (3) is equivalent to the MVDR-like optimization problem [32],

$$\max_{\theta \in [-90^\circ, 90^\circ]} f(\theta) = 1/(\log(\mathbf{a}^H(\theta)\mathbf{R}_{xx}^{-1}\mathbf{a}(\theta)))^2 \tag{4}$$
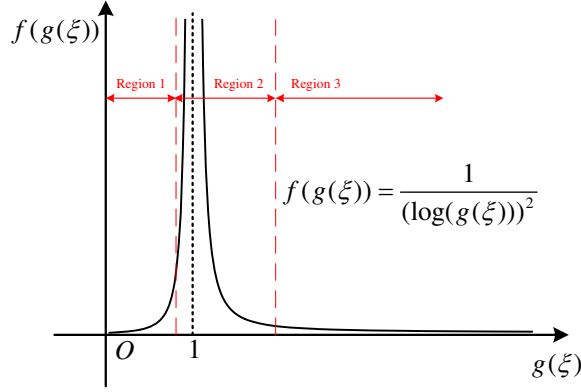
Fig. 1. Diagram of $f(g(\xi)) = 1/(\log(g(\xi)))^2$.

B. Analysis of the IG method

Since (3) and (4) are equivalent, our analysis with respect to different number of sources is based on (4) for simplicity.

Case 1 ($K = 1$):

With the Sherman-Morrison-Woodbury Formula [34], the inverse of $\mathbf{R}_{xx}$ can be expressed as,

$$\begin{aligned}
\mathbf{R}_{xx}^{-1} &= (p_1 \mathbf{a}(\theta_1)\mathbf{a}^H(\theta_1) + \sigma_w^2 \mathbf{I}_M)^{-1} \\
&= \frac{1}{\sigma_w^2}\mathbf{I}_M - \frac{p_1}{\sigma_w^4 + \sigma_w^2 p_1 M}\mathbf{a}(\theta_1)\mathbf{a}^H(\theta_1)
\end{aligned} \tag{5}$$

Then, substituting (5) into $\mathbf{a}^H(\theta)\mathbf{R}_{xx}^{-1}\mathbf{a}(\theta)$, we have

$$\begin{aligned}
g(\xi) &= \mathbf{a}^H(\theta)\mathbf{R}_{xx}^{-1}\mathbf{a}(\theta) \\
&= \frac{M}{\sigma_w^2} - \frac{p_1}{\sigma_w^4 + \sigma_w^2 p_1 M}\mathbf{a}^H(\theta)\mathbf{a}(\theta_1)\mathbf{a}^H(\theta_1)\mathbf{a}(\theta) \\
&= \frac{M}{\sigma_w^2} - \frac{p_1}{\sigma_w^4 + \sigma_w^2 p_1 M}|\xi|^2
\end{aligned} \tag{6}$$

where $|\xi| = \left|\mathbf{a}^H(\theta)\mathbf{a}(\theta_1)\right| = \left|\frac{\sin(M\pi d(sin\theta - \sin\theta_1)/\lambda)}{\sin(\pi d(sin\theta - \sin\theta_1)/\lambda)}\right|$ and $|\cdot|$ gives the amplitude of a complex number. It can be proved that $0 \leq |\xi| \leq M$, and "$=$" holds for $|\xi| = M$ if and only if $\theta = \theta_1$. From (6), we know that $g(\xi)$ is monotonically increasing with respect to $|\xi| \in [0, M]$. Hence, its maximum and minimum are $g_{\max}(\xi) = M/\sigma_w^2$ ($|\xi| = 0$) and $g_{\min}(\xi) = M/(\sigma_w^2 + p_1 M)$ ($|\xi| = M$) .

Given that $f(\theta)$ is not monotonic and as shown in Fig. 1, we redefine the cost function in (4) as $f(\xi) = f(g(\xi)) = 1/(\log(g(\xi)))^2$, and analyze its performance in three different regions:

(Region 1): $g_{\max}(\xi) \leq 1$ (i.e., $\sigma_w^2 \geq M$), the maximum of $f(g(\xi))$ will be achieved at $g(\xi) = g_{\max}(\xi)$, while its minimum is satisfied with $g(\xi) = g_{\min}(\xi)$. That is to say, no matter how large p_1 or SNR is, there will be a deep trough in the IG spectrum for the true DOA θ_1 and several spurious peaks for false θ's which are satisfied with $|\xi| = 0$.

(Region 2): $0 < g_{\min}(\xi) < 1 < g_{\max}(\xi)$ (i.e., $(1 - p_1)M < \sigma_w^2 < M$), $f(g(\xi))$ reaches its maximum when $g(\xi) = 1$. It can be derived that

$$g(\xi) = 1 \Leftrightarrow \frac{M}{\sigma_w^2} - \frac{p_1}{\sigma_w^4 + \sigma_w^2 p_1 M} |\xi|^2 - 1 = 0$$

$$\Leftrightarrow |\xi| = \sqrt{\frac{(M - \sigma_w^2)(p_1 M + \sigma_w^2)}{p_1}} \tag{7}$$

With $(1 - p_1)M < \sigma_w^2 < M$, we have $|\xi| < M$. Then, we can obtain the maximum of $f(g(\xi))$ for $|\xi| < M$. Recalling that $f(g(\xi))$ is quadratic with respect to ξ, there are two different solutions for one single source, i.e., there are two different estimation results $\hat{\theta}_{11}$ and $\hat{\theta}_{12}$ for θ_1, and

$$\left| \mathbf{a}^H(\hat{\theta}_{11}) \mathbf{a}(\theta_1) \right| = \left| \mathbf{a}^H(\hat{\theta}_{12}) \mathbf{a}(\theta_1) \right|$$

$$= \sqrt{\frac{(M - \sigma_w^2)(p_1 M + \sigma_w^2)}{p_1}}$$

$$\Leftrightarrow \sin \theta_1 - \sin \hat{\theta}_{11} = \sin \hat{\theta}_{12} - \sin \theta_1 \tag{8}$$

which means the IG method can result in the spectral splitting phenomenon. In this case, we can obtain the DOA result by averaging the two sine values and calculating its arcsine.

(Region 3): $g_{\min}(\xi) \geq 1$ (i.e., $\sigma_w^2 \leq (1 - p_1)M$), the maximum of $f(g(\xi))$ is reached at $g(\xi) = g_{\min}(\xi)$. Hence, there exists a single peak in the IG spectrum for $\theta = \theta_1$, i.e., a correct estimate. Moreover, since there always exists noise in a real system, i.e., $\sigma_w^2 > 0$, to ensure $\sigma_w^2 \leq (1 - p_1)M$, the power of source signal should be less than one, i.e., $p_1 < 1$.

According to the analysis above, the performance of the IG method is related to the number of array elements, signal power and noise power (not only SNR).

Now we provide some simple simulation results to demonstrate the above analysis. One source signal impinges on a ULA from $\theta_1 = 30°$ with $M = 4$ and $N = 1000$. The settings of p_1 and σ_w^2 are listed in Table I for three different regions. The results are shown in Table I and Fig. 2, which are consistent with the analysis. Furthermore, totally different performances have been obtained with the same SNR, but different signal and noise power values, showing the sensitivity of the IG method. As a result, the IG method can only be applied to some specific scenarios with constraints on M, p_1 and σ_w^2.

TABLE I

PARAMETER SETTINGS AND RESULTS FOR THE IG METHOD WITH A SINGLE SOURCE.

	Region 1	Region 2	Region 3
p_1	50	30	0.9
σ_w^2	5	3	0.09
Results	False	Splitting Spectrum	True

Case 2 $(K = 2)$:

(a) $p_1 = 50$, $\sigma_w^2 = 5$

(b) $p_1 = 30$, $\sigma_w^2 = 3$
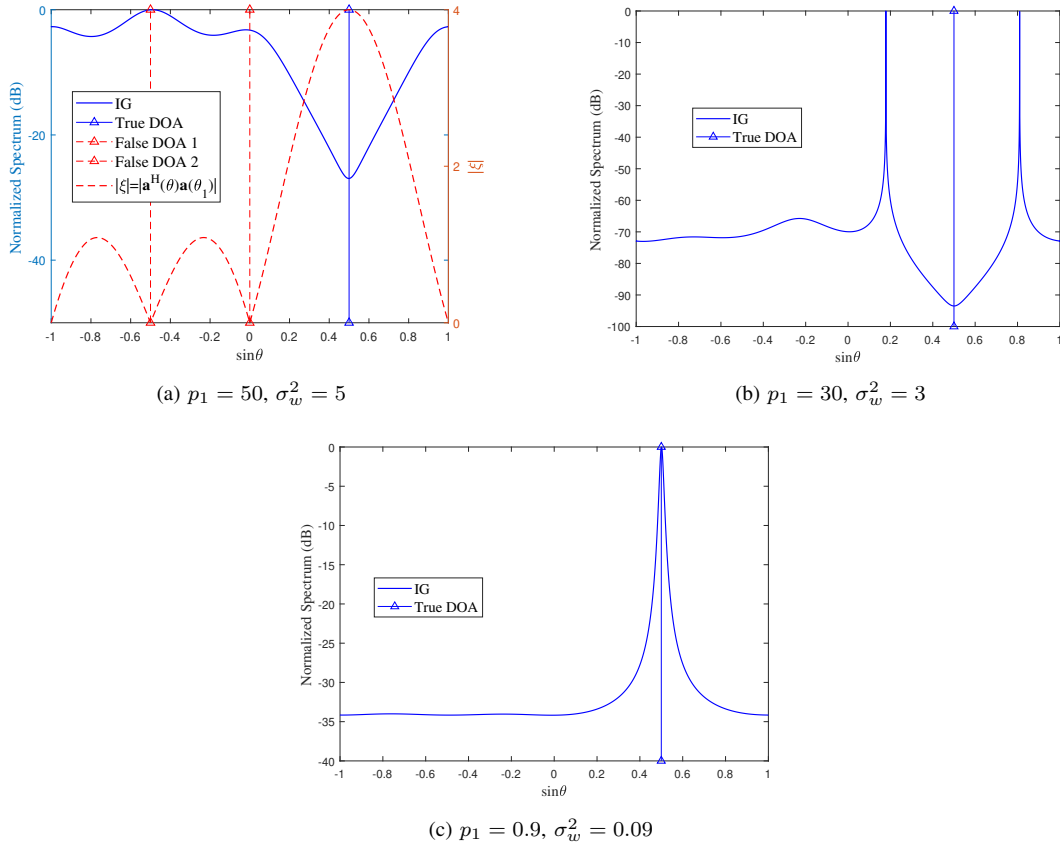
(c) $p_1 = 0.9$, $\sigma_w^2 = 0.09$

Fig. 2. Spectrum for the IG method with a single source in different regions.

Denote the power and DOAs of two sources as p_1, θ_1, p_2, and θ_2, respectively. Similar to (5), we can obtain $\mathbf{R}_{xx}^{-1}$ as follows,

$$
\begin{aligned}
\mathbf{R}_{xx}^{-1} &= (p_1\mathbf{a}(\theta_1)\mathbf{a}^H(\theta_1) + p_2\mathbf{a}(\theta_2)\mathbf{a}^H(\theta_2) + \sigma_w^2\mathbf{I}_M)^{-1} \\
&= \frac{1}{\sigma_w^2}\mathbf{I}_M - \frac{p_1 t_2}{v}\mathbf{a}(\theta_1)\mathbf{a}^H(\theta_1) - \frac{p_2 t_1}{v}\mathbf{a}(\theta_2)\mathbf{a}^H(\theta_2) \\
&\quad + \frac{p_1 p_2 \xi_{12}}{v}\mathbf{a}(\theta_1)\mathbf{a}^H(\theta_2) + \frac{p_1 p_2 \xi_{12}^*}{v}\mathbf{a}(\theta_2)\mathbf{a}^H(\theta_1)
\end{aligned}
\tag{9}
$$

where $\xi_{12} = \mathbf{a}^H(\theta_1)\mathbf{a}(\theta_2)$, $t_1 = \sigma_w^2 + p_1 M$, $t_2 = \sigma_w^2 + p_2 M$, and $v = \sigma_w^2(t_1 t_2 - p_1 p_2 |\xi_{12}|^2)$.

Then, substituting (9) into $\mathbf{a}^H(\theta)\mathbf{R}_{xx}^{-1}\mathbf{a}(\theta)$, we have

$$
\begin{aligned}
g(\xi_1, \xi_2, \xi_{12}) &= \mathbf{a}^H(\theta)\mathbf{R}_{xx}^{-1}\mathbf{a}(\theta) \\
&= \frac{M}{\sigma_w^2} - \frac{p_1 t_2}{v}|\xi_1|^2 - \frac{p_2 t_1}{v}|\xi_2|^2 \\
&\quad + \frac{p_1 p_2 \xi_{12}}{v}\xi_1\xi_2^* + \frac{p_1 p_2 \xi_{12}^*}{v}\xi_1^*\xi_2
\end{aligned}
\tag{10}
$$

where $\xi_1 = \mathbf{a}^H(\theta)\mathbf{a}(\theta_1)$, and $\xi_2 = \mathbf{a}^H(\theta)\mathbf{a}(\theta_2)$.

If M is large, θ_1 is far away from θ_2 and the search angle θ is close to θ_1 or θ_2, $|\xi_{12}|/|\xi_1| \approx 0$ or $|\xi_{12}|/|\xi_2| \approx 0$,

(a) $\theta_1 = 10°$, $\theta_2 = 30°$, $p_1 = p_2 = 3$, $\sigma_w^2 = 3$ (b) $\theta_1 = -10°$, $\theta_2 = 30°$, $p_1 = p_2 = 0.9$, $\sigma_w^2 = 0.09$
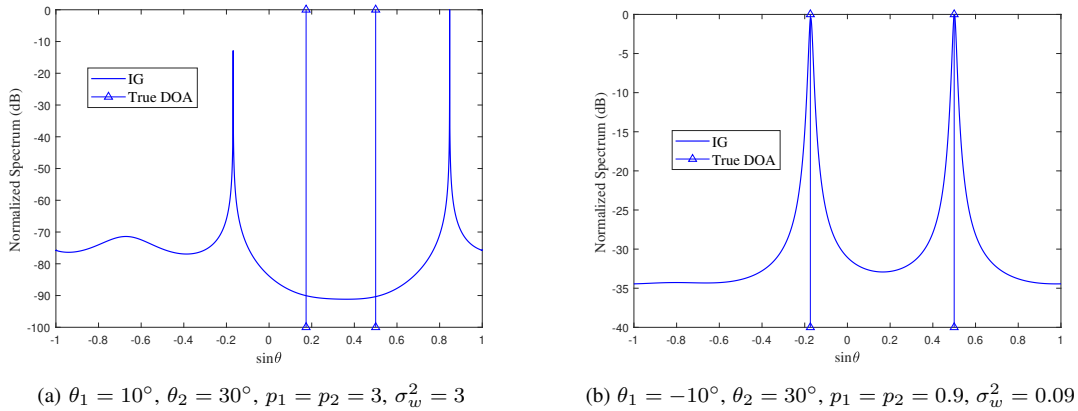
Fig. 3. Spectrum for the IG method with two sources.

and $g(\xi_1, \xi_2, \xi_{12})$ degenerates to $g(\xi_1)$ or $g(\xi_2)$ in (6) and has a similar performance mentioned in case 1 for two sources.

However, if M is small or θ_1 and θ_2 are closely spaced, we can treat $g(\xi_1, \xi_2, \xi_{12})$ as the combination of $g(\xi_1)$, $g(\xi_2)$ and the cross-term corresponding to ξ_{12}. Then, the spectrum of one source will have an effect on that of the other and the cross-term may change one's region. Recall that since each source has three different regions and $0 < g(\xi_1, \xi_2, \xi_{12}) \leq M/\sigma_w^2$, there will be at least five situations. Therefore, we can see that the DOA estimation problem resulting from the IG method is complicated and cannot be dealt with easily by some simple strategies to handle all situations.

Besides, when the two sources belong to region 2, the neighbouring spurious peaks may merge to one or disappear. Importantly, the IG method may result in ambiguity in distinguishing between the case with one source in region 2 and the case with two sources. For clarification, with $M = 4$ and $N = 1000$, simulation results are provided in Figs. 3a -3b. In consideration of Fig. 2b, it is hard to distinguish the differences among the three.

Case 3 ($K \geq 3$):

In this case, the analytical expression of $f(\theta)$ is complicated and it is hard to make quantitative analysis. However, for the special case with some pairs of two closely spaced sources and some isolated single sources, it can be classified into different combinations of case 1 and case 2 with two closely spaced sources, where each combination has a similar performance shown in case 1 and case 2. Its analysis is omitted here.

Overall, as stated in [32], the IG method can provide higher resolution estimation than the MUSIC and MVDR algorithms, but it may result in various ambiguities and even fail for high SNR. Given its unstable performance, a robust and high resolution DOA estimation method using the IG principle is required.

IV. Proposed method

A. Influence of scaling transform on the IG method

Considering the analysis in Section III-B and the nonlinear expression of the IG cost function, we may find an approach, which can change the values of signal and noise power, to tackle the problems of the original IG method. A simple idea is to multiply $\mathbf{x}(n)$ with a positive number η (a scaling transform), i.e.,

$$\tilde{\mathbf{x}}(n) = \eta \mathbf{x}(n) = \eta \mathbf{A}(\theta)\mathbf{s}(n) + \eta \mathbf{w}(n). \tag{11}$$

It is easy to verify that

$$\begin{aligned}
\mathbf{R}_{\tilde{x}\tilde{x}} &= E\{\tilde{\mathbf{x}}(n)\tilde{\mathbf{x}}^H(n)\} \\
&= \sum_{k=1}^{K} \eta^2 p_k \mathbf{a}(\theta_k)\mathbf{a}^H(\theta_k) + \eta^2 \sigma_w^2 \mathbf{I}_M
\end{aligned} \tag{12}$$

Therefore, similar to the analysis in Section III-B, we carry out the estimation using the modified covariance matrix $\mathbf{R}_{\tilde{x}\tilde{x}}$ with respect to different number of sources.

For $K = 1$, with (12), (6) can be expressed as

$$\begin{aligned}
\tilde{g}(\xi) &= \mathbf{a}^H(\theta)\mathbf{R}_{\tilde{x}\tilde{x}}^{-1}\mathbf{a}(\theta) \\
&= \frac{M}{\eta^2 \sigma_w^2} - \frac{p_1}{\eta^2 \sigma_w^2 (\sigma_w^2 + p_1 M)}|\xi|^2
\end{aligned} \tag{13}$$

According to the analysis in Section III-B, to obtain the unambiguous and correct DOA estimation, we should make sure all values of $\tilde{g}(\xi)$ belong to region 3, i.e., $\eta^2 \sigma_w^2 \le (1 - \eta^2 p_1)M$. Then,

$$\eta \le \sqrt{\frac{M}{\sigma_w^2 + p_1 M}} \tag{14}$$

It is noticed that there are infinite number of choices for η. As shown in Fig. 1, since $f(\theta) = f(\tilde{g}(\xi)) = 1/(\log(\tilde{g}(\xi)))^2$ has the steepest slope at $\tilde{g}(\xi) = 1$, we can set $\eta_{\text{opt}} = \sqrt{M/(\sigma_w^2 + p_1 M)}$ to ensure the sharpest spectrum, where the sharper spectrum, the more sensitive to search angles and the better angle estimation performance. Since the estimation of $\mathbf{R}_{\tilde{x}\tilde{x}}$ is usually obtained via $\hat{\mathbf{R}}_{\tilde{x}\tilde{x}} = \frac{1}{N}\sum_{n=1}^{N}\tilde{\mathbf{x}}(n)\tilde{\mathbf{x}}^H(n)$, to avoid $\tilde{g}(\xi)$ located in region 2 resulting from the estimation bias of $\mathbf{R}_{\tilde{x}\tilde{x}}$, we can set η a bit less than η_{opt}, such as $\eta = 0.99\eta_{\text{opt}}$. In addition, it cannot avoid the problem completely for some cases, and we can perform a simple averaging operation to deal with the spectrum splitting problem. Assuming that the two angle estimates of θ being $\hat{\theta}_{11}$ and $\hat{\theta}_{12}$, the final estimate can be obtained as

$$\hat{\theta} = \arcsin\{(\sin\hat{\theta}_{11} + \sin\hat{\theta}_{12})/2\}. \tag{15}$$

Similarly, for $K = 2$, we can express (10) as follows,

$$\begin{aligned}
\tilde{g}(\xi_1, \xi_2, \xi_{12}) &= \mathbf{a}^H(\theta)\mathbf{R}_{\tilde{x}\tilde{x}}^{-1}\mathbf{a}(\theta) \\
&= \frac{M}{\eta^2 \sigma_w^2} - \frac{p_1 t_2}{\eta^2 v}|\xi_1|^2 - \frac{p_2 t_1}{\eta^2 v}|\xi_2|^2 \\
&\quad + \frac{p_1 p_2 \xi_{12}}{\eta^2 v}\xi_1 \xi_2^* + \frac{p_1 p_2 \xi_{12}^*}{\eta^2 v}\xi_1^* \xi_2
\end{aligned} \tag{16}$$

Considering the mutual influence, to avoid spectral splitting and obtain the peaks of $f(\theta) = f(\tilde{g}(\xi_1, \xi_2, \xi_{12})) = 1/(\log(\tilde{g}(\xi_1, \xi_2, \xi_{12})))^2$ at $\theta = \theta_1$ and $\theta = \theta_2$ with the highest resolution, $\tilde{g}(\xi_1, \xi_2, \xi_{12})$ should be equal to 1 for $\theta = \theta_1$ and $\theta = \theta_2$. Moreover, the main purpose here is different from that of the $K = 1$ case, as the $K = 2$ case focuses on the value of $\tilde{g}(\xi_1, \xi_2, \xi_{12})$ for $\theta = \theta_1$ and $\theta = \theta_2$.

When $\theta = \theta_1$, $\xi_1 = M$ and $\xi_2 = \xi_{12}$. Then, we have

$$
\begin{aligned}
& \tilde{g}(\xi_1, \xi_2, \xi_{12}) = 1 \\
\Leftrightarrow & \frac{M}{\eta_1^2 \sigma_w^2} - \frac{p_1 t_2 M^2}{\eta_1^2 v} - \frac{p_2 t_1}{\eta_1^2 v} |\xi_{12}|^2 \\
& + \frac{p_1 p_2 M}{\eta_1^2 v} |\xi_{12}|^2 + \frac{p_1 p_2 M}{\eta_1^2 v} |\xi_{12}|^2 = 1 \\
\Leftrightarrow & \eta_1 = \sqrt{\frac{M t_2 - p_2 |\xi_{12}|^2}{t_1 t_2 - p_1 p_2 |\xi_{12}|^2}}
\end{aligned}
\tag{17}
$$

It can be proved that $0 \le |\xi_{12}| < M$ and η_1 is a monotonically decreasing function of $|\xi_{12}|$ within its effective zone. Therefore, $\sqrt{M/(\sigma_w^2 + p_1 M + p_2 M)} < \eta_1 \le \sqrt{M/(\sigma_w^2 + p_1 M)}$. Additionally, for $\theta = \theta_2$, η_2 has a similar expression as follows,

$$
\eta_2 = \sqrt{\frac{M t_1 - p_1 |\xi_{12}|^2}{t_1 t_2 - p_1 p_2 |\xi_{12}|^2}},
\tag{18}
$$

and $\sqrt{M/(\sigma_w^2 + p_1 M + p_2 M)} < \eta_2 \le \sqrt{M/(\sigma_w^2 + p_2 M)}$.

As shown in (17) and (18), η_1 and η_2 are optimal. But they have complicated relationship with the unknown DOAs and powers of sources and noises, which is hard to utilize directly. However, η_1 and η_2 are determined uniquely, and a criterion can be established using their expressions, which can be utilized to verify if the estimation results are correct or not.

For $K \ge 3$, similar expressions can be derived for the scaling coefficient. However, it is too complicated and may not have any value for practical use, and it is not provided here. Fortunately, the DOA estimation for $K \ge 3$ can be divided into the combination of several $K = 1$ and $K = 2$ problems, which can make full use of the results described above.

B. Proposed method

With the above analysis, we know that estimation of signal and noise power is crucial to the success of the IG method. However, estimation of individual signal powers is a difficult problem. For many conventional applications, the condition that sources have equal or approximately equal powers holds. Hence, as an approximation, we assume all source signals have the same power, i.e., $p_1 = p_2 = \cdots = p_K$. With this assumption, the individual source power can be obtained by estimating their sum. According to the subspace theory, the following results can be

proved

$$\sum_{k=1}^{K} p_k = \sum_{k=1}^{K} \lambda_k - \frac{1}{M-K} \sum_{l=K+1}^{M} \lambda_l, \tag{19}$$

$$\sigma_w^2 = \frac{1}{M-K} \sum_{l=K+1}^{M} \lambda_l, \tag{20}$$

where $\mathbf{R}_{xx} = \sum_{k=1}^{K} \lambda_k \mathbf{u}_k \mathbf{u}_k^H + \sum_{l=K+1}^{M} \lambda_l \mathbf{u}_l \mathbf{u}_l^H$ represents its EVD. The eigenvalues are ordered with $\lambda_1 \geq \lambda_2 \geq \cdots \geq \lambda_K > \lambda_{K+1} = \cdots = \lambda_M$ and $\{\mathbf{u}_k\}_{k=1}^{M}$ are their corresponding eigenvectors.

TABLE II

SUMMARY OF THE PROPOSED METHOD FOR TWO CLOSELY SPACED SOURCES.

---

1. Calculate the covariance matrix $\hat{\mathbf{R}}_{xx} = \frac{1}{N} \sum_{n=1}^{N} \mathbf{x}(n)\mathbf{x}^H(n)$;

2. Apply EVD: $\hat{\mathbf{R}}_{xx} = \sum_{k=1}^{2} \hat{\lambda}_k \hat{\mathbf{u}}_k \hat{\mathbf{u}}_k^H + \sum_{l=3}^{M} \hat{\lambda}_l \hat{\mathbf{u}}_l \hat{\mathbf{u}}_l^H$;

3. Estimate signal and noise powers: $\hat{p}_1 = \hat{p}_2 = \frac{1}{2} \left(\sum_{k=1}^{2} \hat{\lambda}_k - \frac{1}{M-2} \sum_{l=3}^{M} \hat{\lambda}_l \right)$, and $\hat{\sigma}_w^2 = \frac{1}{M-2} \sum_{l=3}^{M} \hat{\lambda}_l$;

4. FOR $\eta \in [\sqrt{M/(\hat{\sigma}_w^2 + \hat{p}_1 M + \hat{p}_2 M)}, \sqrt{M/(\hat{\sigma}_w^2 + \hat{p}_1 M)}]$

    FOR $\theta \in [-90°, 90°]$

        Obtain $\{\hat{\theta}_k\}_{k=1}^{2}$ via searching for spectrum peak of $f(\theta) = 1/\left(\log \left(\frac{1}{\eta^2} \mathbf{a}^H(\theta) \hat{\mathbf{R}}_{xx}^{-1} \mathbf{a}(\theta) \right) \right)^2$;

    END FOR

    Calculate $\varepsilon = \left| \sqrt{\frac{M\hat{t}_2 - \hat{p}_2 |\hat{\xi}_{12}|^2}{\hat{t}_1 \hat{t}_2 - \hat{p}_1 \hat{p}_2 |\hat{\xi}_{12}|^2}} - \eta \right|$ using $\{\hat{\theta}_k\}_{k=1}^{2}$, $\{\hat{p}_k\}_{k=1}^{2}$, and $\hat{\sigma}_w^2$;

    END FOR

5. Obtain the final estimates of $\{\hat{\theta}_k\}_{k=1}^{2}$ when ε reaches its minimum.

To obtain the angle estimation for a single source ($K = 1$), we can use the IG method and the proposed scaling transform with optimum η in (14). For $K = 2$, with the equal signal power assumption and (17)-(18), $\eta_1 = \eta_2$. Hence, only one optimum value $\eta = \eta_1 = \eta_2$ is required to solve. For clarification, the steps of the proposed method are presented in Table II. The key idea is to set a scalar selection condition using the expression of optimum scaling coefficients in (17) and (18), and obtain the optimum value through a linear search. Hence, a robust and satisfactory performance by the proposed method is guaranteed.

As mentioned before, for $K \geq 3$, we may often encounter the case of combination of some pairs of two closely spaced sources and some isolated single sources. In this case, we can use (14) to determine the optimum η for the isolated sources, while use the method in Table II for two closely spaced sources. Specifically, for more than one pair of two closely spaced sources, we can choose an optimum η for one pair each time and treat other pairs as far-away sources. Some initial estimation results may be required to help determine the angle pairs using the conventional methods, such as MVDR [1], MUSIC [4], and IMODE [17]. In addition, the proposed STRING method cannot deal with the case where sources cannot be divided into the combination of some pairs of two closely spaced sources and some isolated single sources, because the proposed method in (11)-(14) and Table II cannot be applied to the case with more than two closely spaced sources.
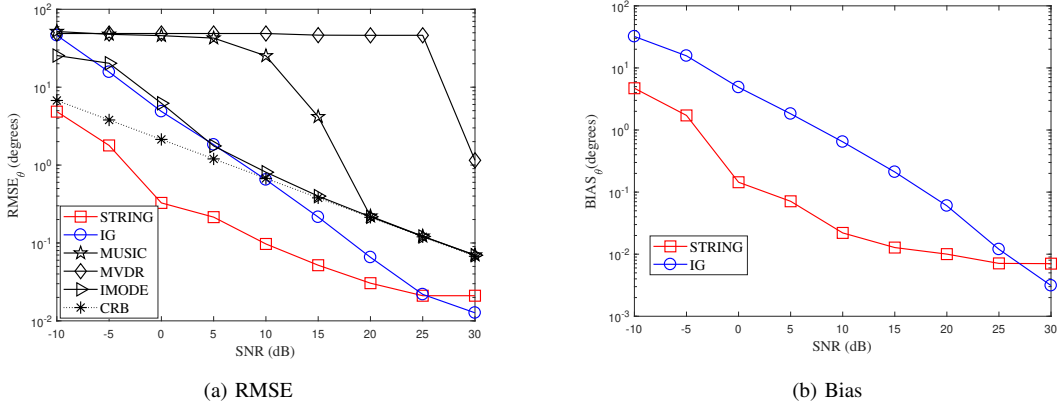
(a) RMSE   (b) Bias

Fig. 4. RMSE and bias versus SNR.

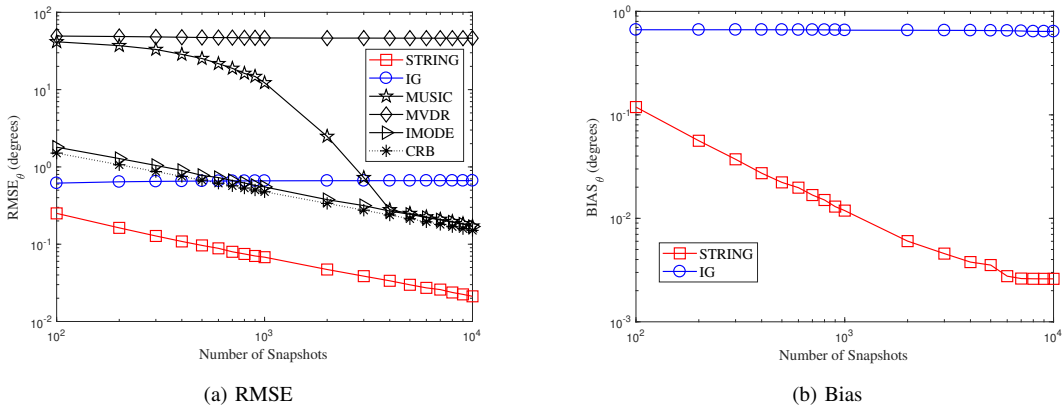(a) RMSE   (b) Bias

Fig. 5. RMSE and bias versus number of snapshots.

V. SIMULATION RESULTS

In this section, we investigate the performance of the proposed method (denoted as 'STRING', short for Scaling TRansform based INformation Geometry) in comparison with that of IG [32], MUSIC [4] , MVDR [1], IMODE [17], and deterministic CRB [8], respectively. It is assumed that $d = \lambda/2$, and the angle search range for all methods is fixed as $[-90°, 90°]$ with an interval of $0.01°$. The search step of η for the proposed method is $1/100$ of the search range. Besides, the signal to noise ratio (SNR) is defined as $\mathrm{SNR} = \mathrm{tr}\{\mathbf{A}(\boldsymbol{\theta})\mathbf{R}_{ss}\mathbf{A}^H(\boldsymbol{\theta})\}/(MK\sigma_w^2)$. The bias and root-mean-square-error (RMSE) of DOA estimates from V Monte Carlo trials, and the corresponding CRB of multiple source signals are calculated as,

$$\mathrm{BIAS}_\theta = \sqrt{\sum_{v=1}^{V}\sum_{k=1}^{K}\left|\hat{\theta}_k^{(v)} - \theta_k\right|/(KV)} \tag{21}$$

$$\mathrm{RMSE}_\theta = \sqrt{\sum_{v=1}^{V}\sum_{k=1}^{K}\left(\hat{\theta}_k^{(v)} - \theta_k\right)^2/(KV)} \tag{22}$$

$$\mathrm{CRB}_\theta = \sqrt{\sum_{k=1}^{K}\mathrm{CRB}_{\theta_k}/K} \tag{23}$$

where $\hat{\theta}_k^{(v)}$ and CRB_{θ_k} denote the estimate of the kth source signal in the vth trial, and the CRB of the kth source signal, respectively.

Example 1: In the first example, we focus on the performance of STRING method under different SNRs. The DOAs and powers of two sources are set to $5°$, $10°$, 1, and 1, respectively. With $M = 4$ and $N = 500$, the SNR varies from -15 dB to 30 dB with an interval of 5 dB. The bias and RSME results are obtained via 1000 Monte Carlo trials for each SNR, shown in Figs. 4a-4b.

From Fig. 4a, we can see that the proposed STRING method has the highest estimation accuracy among all the examined methods for $\mathrm{SNR} \leq 20\mathrm{dB}$ and shows a better performance than the classic CRB, which indicates the excellent resolution ability of the information geometry principle. However, for $\mathrm{SNR} \geq 25\mathrm{dB}$, the original IG method outperforms the STRING method, where the reason may be that the bias resulting from the search accuracy of η using (17) and (18) is larger than that from the cross-term in (10), which indicates that the STRING method is more sensitive to model mismatch errors under very high SNR cases.

As shown in Fig. 4b, although the STRING method obtains a better performance than CRB at the cost of a non-zero bias, the bias is an affordable cost for an improved estimation result.

By the way, we treat the missing DOA estimate as 90 degrees in our Matlab code for convenience, and therefore, RMSEs of about 50 degrees for IG, MUSIC and MVDR occur.

Example 2: In this example, the performance against the number of snapshots is examined. The settings are the same as in Example 1 except that SNR = 10 dB and N ranges from 100 to 10000. The results are provided in Fig. 5a-5b.

As shown in Fig. 5a, the STRING method shows the best performance and is still better than CRB for all values of N considered. Besides, the performance of the original IG method cannot be improved with the increasing number of snapshots, since it does not consider the bias effect of the cross-term in (10). On the other hand, by employing the proposed scaling transform to take into consideration the bias effect, the STRING method has benefited with an improved DOA estimation accuracy. In addition, similar to Example 1, as shown in Fig. 5b, the STRING method is biased.

Example 3: In this example, we investigate the performance under different angle separations. We fix $\theta_1 = 5°$ and change θ_2 with $\Delta\theta = \theta_2 - \theta_1$ from $1°$ to $10°$ with an interval of $1°$. The other settings are the same as in Example 1 except that the SNR = 10 dB. Fig. 6 shows the estimation results, where it can be seen that the STRING method has the best ability to resolve two closely spaced sources.

Example 4: In this example, the performance of the STRING method with respect ot the power difference of two sources is examined. The settings are the same as in Example 1 except that SNR = 10 dB and $p_2 - p_1$ ranges from -10 dB to 10 dB with an interval of 1 dB while p_1 is fixed as 0 dB. The RMSE results are presented in Fig. 7.

As shown, the performance of both STRING and IG varies greatly with the power difference. Specifically, when the power difference of two sources is less than 3dB, STRING can still maintain its excellent performance. Besides, STRING has the highest estimation accuracy when $p_2 - p_1 = 0\mathrm{dB}$, while IG shows the best performance when
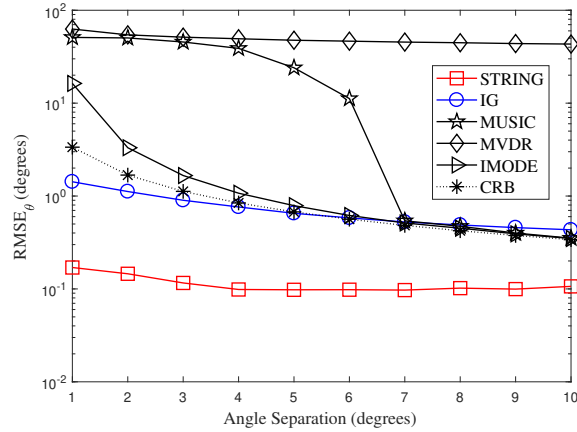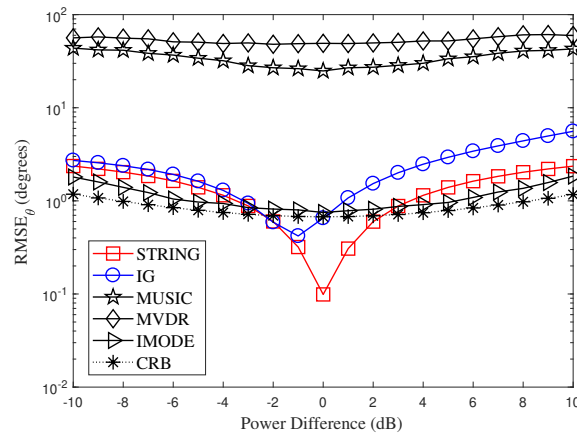
Fig. 6. RMSE versus angle separation.

Fig. 7. RMSE versus power difference.

$p_2 - p_1 = -1\text{dB}$. The reason is that the derivation of STRING is based on the equal power assumption and the cost function of the IG method is nonlinear with respect to source power, which results in the best performance of IG method happening at $p_2 - p_1 = -1\text{dB}$ instead of 0 dB.

Example 5: In this example, we examine the performance of the STRING method for three sources against SNR. Their DOAs and powers are $-30°$, $5°$, $10°$, 1, 1, and 1, respectively. The other settings are the same as in Example 1. The initial estimations for the STRING method are obtained by the IMODE method. Fig. 8 shows the estimation results.

As shown, STRING still has the best performance for three sources when $\text{SNR} \geq 5\text{dB}$ and it can improve the estimation accuracy of the IMODE method. However, the performance of STRING degrades significantly owing to the wrong initial estimations from the IMODE method. Moreover, the IG method cannot preserve its good performance as shown in Example 1 due to the spectrum splitting phenomenon.
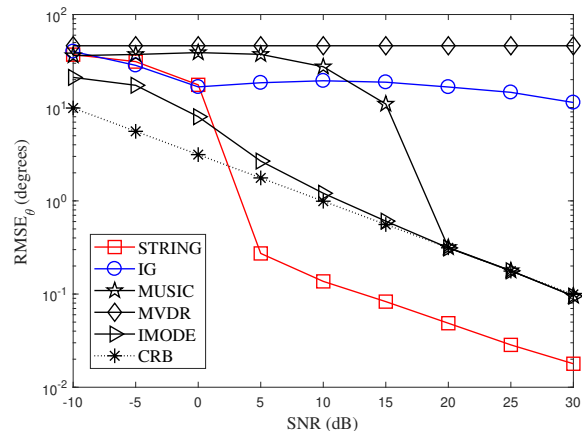
Fig. 8. RMSE versus SNR for three sources.

VI. Conclusions

A robust and high resolution DOA estimation method based on the information geometry principle and a scaling transform has been introduced. A detailed analysis of the original IG method was first provided, showing that the unknown signal and noise parameters, i.e., powers and DOAs of source signals, and noise power, have a great effect on the estimation performance. To tackle the problems encountered by the original IG method, a scaling transform based technique has been introduced and considering the relationship between the optimum scalar with unknown signal DOAs and powers, a linear search based procedure was developed to find the optimum scaling transform. As demonstrated by computer simulations, the so-called Scaling TRansform based INformation Geometry (STRING) method has achieved the best performance for most of the scenarios considered. However, it should be noted that the superior performance of the proposed method is based on the assumption that the source signals have roughly the same power and the source number is known or can be estimated in advance, and further investigation is needed in the future for mixture of strong and weak signals. Besides, the proposed solution for two sources cannot be extended to the case with three or more sources straightforwardly and it has its best performance when two sources are closely spaced with each other.

References

[1] H. L. Van Trees, *Detection, estimation, and modulation theory, optimum array processing*. John Wiley & Sons, 2004.

[2] G.-Q. Zhao, *Principle of Radar Countermeasure*. Xidian University Publisher House, 2nd ed., 2012.

[3] Y. Liu, J. Bo, X. G. Xia, H. Liu, and L. Zhang, "Height measurement of low-angle target using mimo radar under multipath interference," *IEEE Trans. Aerosp. Electron. Syst.*, vol. 54, no. 99, pp. 1–1, 2018.

[4] R. O. Schmidt, "Multiple emitter location and signal parameter estimation," *IEEE Trans. Antennas Propag.*, vol. 34, pp. 276–280, Mar 1986.

[5] R. Roy and T. Kailath, "ESPRIT-estimation of signal parameters via rotational invariance techniques," *IEEE Trans. Acoust., Speech, Signal Process.*, vol. 37, no. 7, pp. 984–995, 1989.

[6] S. Marcos, A. Marsal, and M. Benidir, "The propagator method for source bearing estimation," *Signal Process.*, vol. 42, no. 2, pp. 121–138, 1995.

[7] P. Stoica and K. Sharman, "Maximum likelihood methods for direction-of-arrival estimation," *IEEE Trans. Acoust., Speech, Signal Process.*, vol. 38, no. 7, pp. 1132–1143, 1990.

[8] P. Stoica and A. Nehorai, "MUSIC, maximum likelihood, and Cramer-Rao bound: further results and comparisons," *IEEE Trans. Acoust., Speech, Signal Process.*, vol. 38, no. 12, pp. 2140–2150, 1990.

[9] B. Friedlander, "Sensitivity analysis of the maximum likelihood direction-finding algorithm," *IEEE Trans. Aerosp. Electron. Syst.*, vol. 26, no. 6, pp. 953–968, 1990.

[10] A. K. Seghouane, "A Kullback-Leibler methodology for unconditional ML DOA estimation in unknown nonuniform noise," *IEEE Trans. Aerosp. Electron. Syst.*, vol. 47, no. 4, pp. 3012–3021, 2011.

[11] M. Viberg and B. Ottersten, "Sensor array processing based on subspace fining," *IEEE Trans. Signal Process.*, vol. 39, no. 5, pp. 1110–1121, 1991.

[12] M. Viberg, B. Ottersten, and T. Kailath, "Detection and estimation in sensor arrays using weighted subspace fitting," *IEEE Trans. Acoust., Speech, Signal Process.*, vol. 39, no. 11, pp. 2436–2449, 1991.

[13] I. Ziskind and M. Wax, "Maximum likelihood localization of multiple sources by alternating projection," *IEEE Trans. Acoust., Speech, Signal Process.*, vol. 36, no. 10, pp. 1553–1560, 1988.

[14] M. I. Miller and D. R. Fuhrmann, "Maximum-likelihood narrow-band direction finding and the em algorithm," *IEEE Trans. Acoust., Speech, Signal Process.*, vol. 37, no. 9, pp. 1560–1577, 1990.

[15] Y. Bresler and A. Macovski, "Exact maximum likelihood parameter estimation of superimposed exponential signals in noise," *IEEE Trans. Acoust., Speech, Signal Process.*, vol. 34, no. 5, pp. 1081–1089, 1986.

[16] R. Kumaresan, L. Scharf, and A. Shaw, "An algorithm for pole-zero modeling and spectral analysis," *IEEE Trans. Acoust., Speech, Signal Process.*, vol. 34, no. 3, pp. 637–640, 1986.

[17] P. Stoica and K. C. Sharman, "Novel eigenanalysis method for direction estimation," *IEE Proc. F (Radar, Signal Process.)*, vol. 137, no. 1, pp. 19–26, 1990.

[18] Z. M. Liu, Z. T. Huang, Y. Y. Zhou, and J. Liu, "Direction-of-arrival estimation of noncircular signals via sparse representation," *IEEE Trans. Aerosp. Electron. Syst.*, vol. 48, no. 3, pp. 2690–2698, 2012.

[19] Z. M. Liu, Z. T. Huang, and Y. Y. Zhou, "Array signal processing via sparsity-inducing representation of the array covariance matrix," *IEEE Trans. Aerosp. Electron. Syst.*, vol. 49, no. 3, pp. 1710–1724, 2013.

[20] Z. Yang, J. Li, P. Stoica, and L. Xie, "Chapter 11–sparse methods for direction-of-arrival estimation," *Acad. Press Libr. Signal Process.*, pp. 509–581, 2018.

[21] J. Cai, W. Liu, R. Zong, and B. Wu, "Sparse array extension for non-circular signals with subspace and compressive sensing based DOA estimation methods," *Signal Process.*, vol. 145, 2018.

[22] P. Chevalier, L. Albera, A. Ferreol, and P. Comon, "On the virtual array concept for higher order array processing," *IEEE Trans. Signal Process.*, vol. 53, no. 4, pp. 1254–1271, 2005.

[23] H. Becker, P. Chevalier, and M. Haardt, "Higher order direction finding from rectangular cumulant matrices: the rectangular 2q-MUSIC algorithms," *Signal Process.*, vol. 133, pp. 240–249, 2017.

[24] W.-K. Ma, T.-H. Hsieh, and C.-Y. Chi, "DOA estimation of quasi-stationary signals with less sensors than sources and unknown spatial noise covariance: a Khatri–Rao subspace approach," *IEEE Trans. Signal Process.*, vol. 58, no. 4, pp. 2168–2180, 2010.

[25] M. Y. Cao, L. Huang, C. Qian, J. Y. Xue, and H. C. So, "Underdetermined DOA estimation of quasi-stationary signals via KhatriRao structure for uniform circular array," *Signal Process.*, vol. 106, pp. 41–48, 2015.

[26] Y. Wang, A. Hashemi-Sakhtsari, M. Trinkle, and W. H. Ng, "Sparsity-aware DOA estimation of quasi-stationary signals using nested arrays," *Signal Process.*, vol. 144, pp. 87–98, 2018.

[27] H. Abeida and J.-P. Delmas, "MUSIC-like estimation of direction of arrival for noncircular sources," *IEEE Trans. Signal Process.*, vol. 54, no. 7, pp. 2678–2690, 2006.

[28] Y. Shi, L. Huang, C. Qian, and H. C. So, "Direction-of-arrival estimation for noncircular sources via structured least squaresbased esprit using three-axis crossed array," *IEEE Trans. Aerosp. Electron. Syst.*, vol. 51, no. 2, pp. 1267–1278, 2015.

[29] H. Chen, C. Hou, W. P. Zhu, W. Liu, Y. Y. Dong, Z. Peng, and Q. Wang, "ESPRIT-like two-dimensional direction finding for mixed circular and strictly noncircular sources based on joint diagonalization," *Signal Process.*, vol. 141, pp. 48–56, 2017.

[30] P. Pal and P. Vaidyanathan, "Nested arrays: A novel approach to array processing with enhanced degrees of freedom," *IEEE Trans. Signal Process.*, vol. 58, no. 8, pp. 4167–4181, 2010.

[31] P. P. Vaidyanathan and P. Pal, "Sparse sensing with co-prime samplers and arrays," *IEEE Trans. Signal Process.*, vol. 59, no. 2, pp. 573–586, 2011.

[32] M. Coutino, R. Pribic, and G. Leus, "Direction of arrival estimation based on information geometry," in *Int. Conf. Acoust., Speech, Signal Process. (ICASSP)*, pp. 3066–3070, IEEE, 2016.

[33] S. T. Smith, "Covariance, subspace, and intrinsic Cramer-Rao bounds," *IEEE Trans. Signal Process.*, vol. 53, no. 5, pp. 1610–1630, 2005.

[34] H. V. Henderson and S. R. Searle, "On deriving the inverse of a sum of matrices," *SIAM Review*, vol. 23, no. 1, pp. 53–60, 1981.

Yang-Yang Dong was born in Bengbu, Anhui, China. He received the B.Eng. and Ph.D. degrees in Electronic Science and Technology from Xidian University, Xian, China, in 2012 and 2017, respectively. Since 2017, he has been a Lecturer with the School of Electronic Engineering, Xidian University, where he also held a post-doctoral position. His current research interests include array signal processing, multilinear algebra, and information geometry.

Chun-Xi Dong was born in Sanmenxia, Henan, China. He received the Ph.D. degree from Xidian University, in 2004. He is currently an Associate Professor and the Director of the Information Technology Department, School of Electronic Engineering, Xidian University. His current research interests include high speed signal processing and system simulation.

Wei Liu (S'01-M'04-SM'10) received his BSc and LLB. degrees from Peking University, China, in 1996 and 1997, respectively, MPhil from the University of Hong Kong in 2001, and PhD from the School of Electronics and Computer Science, University of Southampton, UK, in 2003. He then worked as a postdoc first at Southampton and later at the Department of Electrical and Electronic Engineering, Imperial College London. Since September 2005, he has been with the Department of Electronic and Electrical Engineering, University of Sheffield, UK, first as a Lecturer and then a Senior Lecturer. He has published more than 270 journal and conference papers, five book chapters, and two research monographs titled "Wideband Beamforming: Concepts and Techniques" (John Wiley, March 2010) and "Low-Cost Smart Antennas" (by Wiley-IEEE, March 2019), respectively. His research interests cover a wide range of topics in signal processing, with a focus on sensor array signal processing (beamforming and source separation/extraction, direction of arrival estimation, target tracking and localisation, etc.), and its various applications, such as robotics and autonomous systems, human computer interface, radar, sonar, satellite navigation, and wireless communications.

He is a member of the Digital Signal Processing Technical Committee of the IEEE Circuits and Systems Society and the Sensor Array and Multichannel Signal Processing Technical Committee of the IEEE Signal Processing Society (Vice-Chair from Jan 2019). He was an Associate Editor for IEEE Trans. on Signal Processing (March 2015-March 2019) and is currently an Associate Editor for IEEE Access, and an editorial board member ofthe Journal Frontiers of Information Technology and Electronic Engineering.

Ming-Ming Liu was born in Ningxia, China. She received the M.Eng. degree in Electronic Science and Technology from Xidian University, Xian, China, in 2016, where she is currently pursuing the Ph.D. degree in electronic science and technology. Her research interests include compressed sensing, and array and radar signal processing.

Zheng-Zhao Tang was born in Baoji, Shaanxi, China. He received the B.Eng. degree in Electronic Science and Technology from Xidian University, Xian, China, in 2014, where he is currently pursuing the Ph.D. degree with the School of Electronic Engineering. His current research interests include inverse synthetic aperture radar imaging and its countermeasure technology.